Low-optical-pumping-threshold InGaAs/GaAs nano-ridge laser monolithically grown on 300 mm silicon substrate

Z. Ouyang,[1] E. M. B. Fahmy,[1] D. Colucci,[1,2] A. A. Yimam,[1] B. Kunert[2] and D. Van Thourhout[1]

[1] *Gent University-imec, Photonics Research Group, INTEC department, iGent, Technologiepark-Zwijnaarde 126, 9052 Ghent, Belgium*
[2] *IMEC, Kapeldreef 75, 3001 Heverlee, Belgium*

Abstract: Amorphous-silicon-grating-on-top DFB-laser directly grown on silicon substrate by nano-ridge engineering technique exhibits 2.5 kW/cm^2 lasing threshold, 10 times smaller than nano-ridge laser with etched grating, due to avoiding introducing carrier loss path at GaAs-air surface.

1. Introduction

Leveraging well-developed processes from the complementary metal-oxide semiconductors (CMOSs) industry, silicon photonics circuits incorporating various optical components, including high-efficiency grating couplers, high-response-speed photodetectors and excellent modulators[2-4] are now widely studied. However, the lack of a high-performance laser is a main bottleneck for further development of the silicon photonic platform. Direct-bandgap III-V semiconductors are the promising candidate for realizing a practical and compact light source but not easy to integrated on silicon. Several methods, including flip-chip, bonding, transfer printing and direct epitaxy of III-V materials utilizing a buffer layer[5-8], were explored to achieve this but all have their limitations. The novel nano-ridge engineering (NRE) technique[9-10] has been shown to enable the growth of high-quality III-V material directly on Si substrates without any buffer layer, and compared to other methods shows advantages in terms of device scalability, integration density and cost.

In our previous work, although the nano-ridge cavity with etched grating had been realized, the threshold of these devices were still high[1]. One of the reasons is that the etched structure caused the damage to InGaP passivation layer, which introduces additional carrier loss path at the GaAs-air surface. Therefore, in this work, high-refractive-index, but 'weak' and small amorphous silicon (a-Si) grating were deposited on the top of nano-ridge rather than etched grating inside nano-ridge. The design of a-Si grating considered the light interaction with grating and more mode overlap with quantum wells into account, contributing to form nano-ridge cavity with low lasing turn-on behavior.

2. Results and discussion

After optimizing the trade-off between light interaction with the a-Si grating on the top of the nano-ridge and mode confinement in quantum wells with a 3D-finite difference time domain (3D-FDTD) solver, 539 nm-high nano-ridge distributed feedback (DFB) laser was fabricated with 100 nm-thick, 161 nm-period and 800-period a-Si grating on the top. Figure 1(a) and (b) present zoomed-in tilted scanning electron microscope (SEM) images of the DFB laser and the view of vertical sidewall and smooth surface of the a-Si grating, which benefit the low-optical-pumping-threshold. The same device was excited by a Nd:YAG 532-nm nanosecond pulsed laser at room temperature and the emission from the devices was collected and detected with a monochromator and a thermo-electric-cooled InGaAs detector. Figure 1(c) shows the photoluminescence spectrum of this device under different 532nm pulsed pumping power densities. The 1044 nm lasing peak becomes apparent when the pumping density reaches 2.5 kW/cm^2 in the inset and the peak intensity increases strongly with the further increase of the pumping density. At the pumping power density of 35 kW/cm^2, the lasing peak reaches more than 35 dB side-mode suppression ratio and the linewidth of the laser is 1.5 nm limited by carrier dispersion during the pulsed operation regime, which demonstrate excellent laser performance.

Figure 1(d) shows the same measured device light in (pumping power density) - light out (integrated photoluminescence intensity) curve on logarithm and linear (inset) scale. A clear change of slope indicates strongly the lasing turn-on behavior. The fitting of measured output light intensity versus pumping power density is performed with the rate equations in the open cavity model[11-12]. The fitting gives the value of coupling efficiency from the spontaneous emission to the cavity mode $\beta \sim 2.66\%$, around 3 times larger than the one in the cavity with etched gratings. Excited electron-hole pairs are mostly coupled with free-space modes when the pumping power density is lower than threshold and the cavity mode photons can only increase rapidly above "threshold" because of intensive stimulated emission. Additionally, the increase of β value is smaller than the decrease of the lasing turn-on

threshold value. This indicates that another carrier loss path is prevented to help for the further reduction of threshold value. For understanding the reason of lowering threshold further, the carrier loss mechanism should be investigated in the future work.

Figure 1(a) The tilted SEM image of a 539 nm-high nano-ridge DFB laser. (b) The zoomed-in tilted SEM image of the a-Si grating on the top of the same nano-ridge laser. (c) Photoluminescence spectrum from the same 539 nm-high nano-ridge DFB laser under different 532 nm pulsed pumping densities. Inset: Photoluminescence spectrum from the same DFB laser under 2.5 kW/cm^2 pulsed pumping density (d) Light in (pumping power density) -Light out (integrated photoluminescence intensity) curve on linear (inset) and logarithmic scale of the same DFB laser.

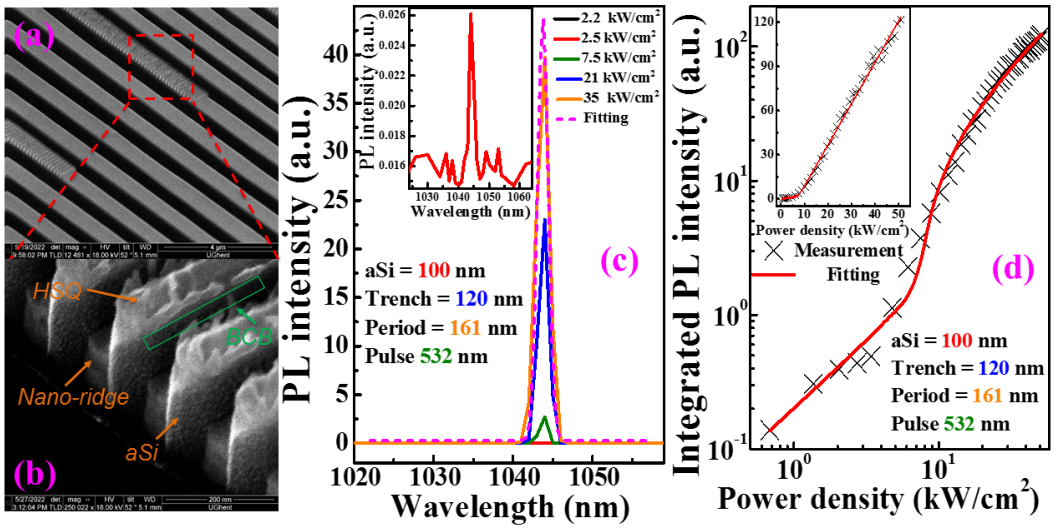

3. References

[1] Y. Shi, Z. Wang, J.V. Campenhout, et al, "Optical pumped InGaAs/GaAs nano-ridge laser epitaxially grown on a standard 300-mm Si wafer", Optica **4**, 1468-1473 (2017).

[2] R. marchetti, C. Lacava, A. khokhar, et al, "High-efficiency grating-couplers:demonstration of a new design strategy", Sci. Rep. **7**, 16670:1-8 (2017).

[3] N. Youngblood, C. Chen, S. J. Koester and M. Li, "Waveguide-integrated black phosphorus photodetector with high responsivity and low dark current", Nature Photon. **9**, 247-252 (2015).

[4] Y. Terada, K. Kondo, R. Abe and T. Baba, "Full C-band Si photonic crystal waveguide modulator", Opt. Lett. **42**, 5110-5112 (2017).

[5] H. Lu, J. Lee, Y. Zhao et al, "Flip-chip integration of tilted VCSELs onto a silicon photonic integrated circuit", Opt. Express **42**, 5110-5112 (2017).

[6] M. R. Billah, M. Blaicher, T. Hoose, et al, "Hybrid integration of silicon photonics circuits and InP lasers by photonic wire bonding", Optica **5**, 876-883 (2018).

[7] J. Zhang, G. Muliuk, J. Juvert, et al, "III-V-on-Si photonic integrated circuits realized using micro-transfer-printing", APL Photonics **4**, 11803:1-10 (2019).

[8] J. Yang, P. Jurczak, F. Cui, et al, "Thin Ge buffer layer on silicon for integration of III-V on silicon", J. Cryst. Growth **514**, 109-113 (2019).

[9] B. Kunert, W. Guo, Y. Mols, et al, "Integration of III/V Hetero-Structures by Selective Area Growth on Si for Nano- and Optoelectronics", ECS Trans. **35**, 679-681 (2010).

[10] B. Kunert, R. Alcotte, Y. Mols, et al, "Application of an Sb Surfactant in InGaAs Nano-ridge Engineering on 300 mm Silicon Substrates", Cryst. Growth Des. **21**, 1657-1665 (2021).

[11] H. Yokoyama and S. D. Brorson, "Rate equation analysis of microcavity lasers", J. Appl. Phys. **66**, 4801 (1989).

[12] K. A. Shore and M. Ogura, "Threshold characteristics of microcavity emiconductor lasers", Opt. and Quantum Electron. **24**, 209-213 (1992).